



TITLE:

Groundwater dating by estimation of groundwater flow velocity and dissolved ^4He accumulation rate calibrated by ^{36}Cl in the Great Artesian Basin, Australia

AUTHOR(S):

Mahara, Yasunori; Habermehl, M.A.; Hasegawa, T.; Nakata, K.; Ransley, T.R; Hatano, T.; Mizuochi, Y.; ... Senior, B.R.; Yasuda, H.; Ohta, T.

CITATION:

Mahara, Yasunori ...[et al]. Groundwater dating by estimation of groundwater flow velocity and dissolved ^4He accumulation rate calibrated by ^{36}Cl in the Great Artesian Basin, Australia. *Earth and Planetary Science Letters* 2009, 287(1-2): 43-56

ISSUE DATE:

2009-09

URL:

<http://hdl.handle.net/2433/86183>

RIGHT:

c 2009 Elsevier B.V.; This is not the published version. Please cite only the published version.; この論文は出版社版ではありません。引用の際には出版社版をご確認ご利用ください。

Groundwater dating by estimation of groundwater flow velocity and
dissolved ^4He accumulation rate calibrated by ^{36}Cl
in the Great Artesian Basin, Australia

Y. Mahara^{a*}, M. A. Habermehl^b, T. Hasegawa^c, K. Nakata^c, T. R. Ransley^b, T. Hatano^d,
Y. Mizuochi^e, H. Kobayashi^e, A. Ninomiya^e, B. R. Senior^f, H. Yasuda^g and T. Ohta^a

a: Research Reactor Institute, Kyoto University, Kumatori, Osaka 590-0494, Japan.

b: Integrated Water Sciences Program, Bureau of Rural Sciences, Canberra, A. C. T.,
2601, Australia.

c: Central Research Institute of Electric Power Industry, Abiko, Chiba 270-1194, Japan.

d: Dept. Engineering Industry, J. Power, Ginza, Tokyo 104-8165, Japan.

e: Tech. Res. Dept. Sumiko Consultants Co. Ltd., Taito, Tokyo 110-0008, Japan.

f: B. R. Senior & Assoc. Pty Ltd., Bungendore, N.S.W., Australia.

g: Research Center for Radiation Protection, National Institute of Radiological Sciences,
Anagawa, Chiba 263-8555, Japan

*: Corresponding author, Tel. +81-724-51-2462, Fax. +81-724-51-2636,

E-mail: mahara@ rri.kyoto-u.ac.jp

Abstract

We tested two methods for dating groundwaters that cannot be reliably measured by ^{36}Cl dating alone, one based on groundwater flow velocity plus distance along a flow path and the other based on ^4He accumulation rates calibrated with ^{36}Cl dates. We sampled groundwaters along six inferred regional groundwater flow paths in the Great Artesian Basin (GAB) of Australia. We selected three groundwater paths where the decrease in ^{36}Cl was largely controlled by cosmogenic ^{36}Cl radioactive decay without a significant increase in chloride concentration. The extrapolated groundwater velocities were 0.133 ± 0.018 m/y to 0.433 ± 0.140 m/y. The estimated residence time of 1.06×10^6 y at the discharge area around Lake Eyre was comparable to the estimate of $(1\text{--}2.2) \times 10^6$ y in previous studies. On the other hand, our estimated ^4He accumulation rates for the selected three groundwater flow paths ($1.85 \pm 0.31 \times 10^{-11}$ to $1.51 \pm 0.63 \times 10^{-10}$ ccSTP/cm 3 ·y) were approximately 2–15 times lower than previously reported rates for the central GAB. Our estimated rate of 1.51×10^{-10} ccSTP/cm 3 ·y $^{-1}$ in the western GAB is compatible with previous estimates based on ^{81}Kr ages. The groundwater residence time estimated from the ^4He accumulation rate was approximately 7×10^5 y near the discharge area at Lake Eyre. Finally, both estimations were mutually compatible with a 30% error.

Keywords: GAB; ^4He accumulation; environmental tracer; cosmogenic ^{36}Cl ; subsurface produced ^{36}Cl ; chloride concentration; evapotranspiration

1. Introduction

Disposal of high-level radioactive waste in stable, deep geological strata is an area of active research. In safety assessments, groundwater flow is the most important factor in transporting radionuclides released from wastes to the biosphere. Radioactive wastes should be placed in a site where groundwater flow is very low or stagnant. However, groundwater flow velocities of less than a few centimeters per year cannot be measured using conventional techniques. Yet a groundwater travel or residence time on the order of 1 million years must be determined to judge whether groundwater movement at a candidate disposal site is acceptable.

Various methods have been proposed for dating groundwater [1, 2]. Most of these rely on environmental tracers, including radioisotopes, stable isotopes, and chemicals dissolved in groundwater. Few have been verified in well-studied extended groundwater flow paths or compared with proven methods. Recently, Bethke and Johnson [3] summarized theoretical problems and applications to groundwater age and dating of the piston flow model and the reactive transport model. They suggested that dissolved excess ^4He concentration is a direct proxy for groundwater age in the Great Artesian Basin (GAB), Australia. However, the estimation of groundwater age from the reactive transport model that they favored is based on detailed simulation results using a hypothetical flow regime.

We propose two simple estimation methods that use piston flow models based on radiological decay of cosmogenic ^{36}Cl and the addition of autochthonously produced (geogenic) ^{36}Cl . The proposed methods, one based on extrapolation of groundwater flow velocity and the other using the accumulation rate of ^4He calibrated against the radiological curves of cosmogenic and geogenic ^{36}Cl , may extend groundwater dating to unprecedented ages. We collected groundwater samples along several groundwater flow paths in the GAB, a well-studied confined aquifer system considered ideal for verifying dating methods, and compared the results with those of previous studies [3–11].

In this study, we selected groundwater flow paths and sampling sites in the GAB to calibrate our proposed dating methods, which made it possible to measure residence times greater than 10^6 y, beyond the range of results considered reliable by ^{36}Cl dating. We extrapolated the optimum

groundwater flow velocity and ^4He accumulation rate in the selected groundwater flow paths on the basis of ^{36}Cl dating and using a preliminary analytical simulation and investigations of the groundwater origin and hydrochemical evolution trends [12, 13].

2. Description of the Study Area and Simulated Distribution Results of the ^4He Concentration and $^{36}\text{Cl}/\text{Cl}$ Ratio

We selected 77 water-bores (wells) and 2 artesian springs in the GAB and collected groundwater samples from them during 2002 and 2003. The water-bores met three criteria: (1) Bores tapped the confined aquifer in the Lower Cretaceous to Jurassic Cadna-owie Formation and Hooray Sandstone or their equivalents, which extend across the whole basin [14–16]. (2) Bores were flowing water-bores, and nearly all have flowed continuously for many decades, although several samples were collected from pumped water-bores in recharge areas. (3) Bores were distributed along the entire length of six regional groundwater flow paths within the Cadna-owie Formation–Hooray Sandstone aquifer (Fig. 1); these flow paths extend from recharge to discharge areas and avoid mixing with groundwater from other aquifers. We selected water-bores aligned with the groundwater flow lines that were inferred by Welsh [17], Habermehl [14] and Habermehl and Lau [16] (see Figure 11 in Radke et al. [18]).

We analyzed the distribution of dissolved ^4He concentration and $^{36}\text{Cl}/\text{Cl}$ ratio in groundwater using a three-dimensional aquifer model [12]. We modeled the Cadna-owie Formation–Hooray Sandstone aquifer, bounded at top and bottom by impermeable aquitards, in the entire GAB with five vertical layers and 74,655 horizontal $10\text{ km} \times 10\text{ km}$ grid cells. Groundwater flow was analyzed under steady-state condition using conductivities between approximately 1×10^{-5} and $1 \times 10^{-6}\text{ m/s}$ and porosity of 25%. Transport of dissolved ^4He and ^{36}Cl was analyzed, based on the distribution of groundwater flow velocity, by using dispersivity values of 10 km longitudinal and 2 km transverse, diffusion coefficients of $10^{-5}\text{ cm}^2/\text{s}$, bottom ^4He flux of $2 \times 10^{-9}\text{ m}^3/\text{m}^2\text{ y}^{-1}$, an ^4He in situ production rate of $1 \times 10^{-12}\text{ ccSTP/g}_w\text{y}^{-1}$, initial $^{36}\text{Cl}/\text{Cl}$ ratio of 130×10^{-15} , and secular equilibrium $^{36}\text{Cl}/\text{Cl}$ ratio of 5×10^{-15} . All analyses were conducted by the finite-element method. The observed contours of ^4He concentration and $^{36}\text{Cl}/\text{Cl}$ ratio were drawn by the kriging method based on the measured values. We

show the comparisons between observations of dissolved ^4He concentration and $^{36}\text{Cl}/\text{Cl}$ ratio and analytical results for ^4He ratio and $^{36}\text{Cl}/\text{Cl}$ concentration in the aquifer in Figs. 2 and 3. The ^4He analysis generally reproduced the distribution of observed ^4He concentrations except in the central zone of the basin, where the dissolved He concentration was reduced by intense degassing of ^4He owing to boiling at approximately 100 °C and releasing from high pressure at the well head. The $^{36}\text{Cl}/\text{Cl}$ analysis also reproduced the observed $^{36}\text{Cl}/\text{Cl}$ distribution in the GAB except in the marginal discharge zone and the western recharge zone owing to the invasion of high saline water from an underlying marine layer.

3. Results and Discussion

Table 1 lists distances of the water-bores along the six regional groundwater flow lines published in previous detailed studies [14–19], which are also supported by groundwater flow analyses and backtracking analysis conducted by Hasegawa [12]. Distances were measured along the inferred flow line from the recharge zone to the water-bore. Table 2 lists isotopic data from the samples. In addition, the aquifer rock was sampled in five places (Fig. 1) and analyzed for levels of relevant radiogenic elements (U, Th, Li), neutron flux, helium production, and He and Cl isotopes; these results are shown in Table 3. We have detailed our analytical methods for dissolved He and Ne, tritium, U and Th content in rock, and $^{36}\text{Cl}/\text{Cl}$ ratio elsewhere [20].

3.1 Hydrochemical and stable isotopic characteristics of groundwater

Distribution of the major cations (Na^+ , K^+ , Ca^{2+} , and Mg^{2+}) and anions (Cl^- , HCO_3^- , and SO_4^{2-}) have already been discussed and these differences are detailedly documented in earlier publications by Habermehl [14,15] and Radke et al. [18]. We also confirmed these distribution and differences [13]. The artesian groundwater in most of the GAB is characterized by Na-HCO_3 or $\text{Na-HCO}_3\text{-Cl}$, and the western part is characterized by Na-Cl-SO_4 . Total dissolved ion concentrations in the western GAB are greater than those in the other parts. Concentrations of dissolved major ions in the western areas increase roughly with distance along flow lines from the recharge zones.

We plotted all data for stable isotopes (D and ^{18}O) in Fig. 4. This figure includes two different correlation lines. Most of the data from regional groundwater flow paths A, B, and C in the central GAB are aligned along the upper correlation line ($\delta \text{D} = 4.63 \pm 0.34 \times \delta ^{18}\text{O} - 10.3 \pm 2.3$; $r^2 = 0.895$) and data from paths D and E in the western GAB align along the lower line ($\delta \text{D} = 5.69 \pm 0.28 \times \delta ^{18}\text{O} - 11.06 \pm 2.1$; $r^2 = 0.949$). This result suggests that groundwater was recharged at the eastern margin of the GAB for paths A, B, and C and at the western margin for paths D and E. Data from flow path F and the discharge part of flow path D plotted between these two correlation lines. As path F is located at the ridge between the central and the western GAB, groundwater was probably affected by mixing. Groundwater was similarly mixed in the discharge zone on path D. Furthermore, the slopes of the two correlation lines, 4.63 ± 0.34 and 5.69 ± 0.28 , respectively, are significantly smaller than that of the global meteoric water line. This suggests contributions by evapotranspiration or ion filtration. However, because the slope for ion-filtration effects should be approximately 3.1 according to Coplen and Hanshaw [21], the probability of ion filtration is low. Evapotranspiration would account for a local variation of stable isotopes in the recharge areas in both the eastern and western margins of the GAB, as mentioned by Love et al. [9]

3.2 Selection of groundwater flow paths deduced from the correlation between $^{36}\text{Cl}/\text{Cl}$ ratio and the inverse of the chloride concentration

We analyzed the correlation between the ratio $^{36}\text{Cl}/\text{Cl}$ and $1/\text{Cl}$ in a set of mixing curves using two different groundwaters as end members with different salinities and different $^{36}\text{Cl}/\text{Cl}$ ratios. The results of six mixing cases are plotted in Fig. 5.

Our results indicate that the decrease in ^{36}Cl atoms along three short flow paths (A, C, and D) was strongly controlled by radioactive decay rather than by mixing with other groundwater flows and diffusion from aquitards, because $^{36}\text{Cl}/\text{Cl}$ ratios not only did not fall on a single mixing line but also fell perpendicularly independent of the inverse chloride concentration, except near where $^{36}\text{Cl}/\text{Cl}$ ratios reached their secular value ($<10^{-14}$). This suggests that very little added chloride dissolved or diffused from the aquifer rock matrix or the aquitards, which is at a secular equilibrium condition for

the $^{36}\text{Cl}/\text{Cl}$ ratio. These results agree with the suggestion that the ^{36}Cl concentration is in line with predictions from the piston flow model and from the reactive transport model near the recharge zone [3].

On path E, the $^{36}\text{Cl}/\text{Cl}$ ratio appeared to be almost independent of changes in chloride concentration. This suggests that chloride concentration is controlled by severe evapotranspiration of infiltrating water in the thick unsaturated recharge zone in the western GAB, as reported by Love et al. [9] and our result from stable isotope observations shown in Fig. 4. As condensation of chloride would occur during rainwater infiltration into the unsaturated zone in a short period, the reduction effects do not appear to have been caused by radioactive decay of ^{36}Cl . Also, a significant amount of ^{14}C was detected on this flow path, but not on the other flow paths, which indicates a short residence time compared with the half-life of ^{36}Cl . Paths B and F are both exceptionally long flow lines. Both paths have order-of-magnitude differences in their inverse chloride concentrations ($1/\text{Cl}$) over the range of $^{36}\text{Cl}/\text{Cl}$ ratios, owing to mixing between different flow paths with different origins as well as dissolution and diffusion of chloride over long distances. This is fully consistent with the findings of previous studies [3–13, 18].

Consequently, we selected paths A, C, and D, in which mixing and diffusion effects were negligible, for further analyses based on ^{36}Cl dating. These flow paths display a relatively good correlation between the $^{36}\text{Cl}/\text{Cl}$ ratio and dissolved ^4He concentration, which is expected to be equivalent to elapsed time, as shown in Fig. 6. In other words, $^{36}\text{Cl}/\text{Cl}$ ratios decrease with increasing dissolved ^4He concentration by the same exponential function as radioactive decay: $^{36}\text{Cl}/\text{Cl} = \exp [(4.8401 \pm 0.15548) + (-62928.5 \pm 11251.6) \times ^4\text{He}]$, ($r^2 = 0.73353$) for path A, $^{36}\text{Cl}/\text{Cl} = \exp [(4.56927 \pm 0.10445) + (-33811.0 \pm 8066.3) \times ^4\text{He}]$, ($r^2 = 0.70301$) for path C, and $^{36}\text{Cl}/\text{Cl} = \exp [(4.74142 \pm 0.19206) + (-20326.3 \pm 6052.7) \times ^4\text{He}]$, ($r^2 = 0.56231$) for path D.

3.3 Setting chlorine parameters for calibration using ^{36}Cl

We set some key chlorine parameters for ^{36}Cl dating using our own measured data in this field work campaign and referred values in previous published data [3,5,6,9,11-14,18].

We measured chloride concentration in groundwaters across the GAB. The initial chloride concentration in the recharge zone in the central GAB ranged from 27 to 178 mg/L. Bentley et al. [5] reported an initial chloride concentration of 64 mg/L, and Torgersen et al. [6] used both 64 mg/L and 30 mg/L for initial values in analyses of ^{36}Cl dating in the central GAB. In this study, we chose 20 mg/L, based on the lowest value in Table 1, as the initial chloride concentration in the central GAB considering condensation of chloride by strong evapotranspiration. We conducted parameter sensitivity analyses using initial chloride concentrations of 20, 64, and 100 mg/L for the analyses of groundwater velocity and ^4He accumulation rate, but found no significant effect. There were no significant differences in the initial chloride concentration among 20, 64, and 100 mg/L from the

$$\text{correlation between the term of } \left(\frac{R_m - R_{eq}}{R_0 - R_{eq}} \right) \cdot \left(\frac{Cl_m}{Cl_0} \right)$$

where, Cl_0 and R_0 are the initial value of the chlorine concentration and the initial $^{36}\text{Cl}/\text{Cl}$ ratio, respectively, in rainwater infiltrated in the recharge zone; R_{eq} is the secular equilibrium $^{36}\text{Cl}/\text{Cl}$ ratio in the aquifer and aquitard.

and the flow distance L and ^4He concentration for paths A and C. Judging from stable isotope data and measured chloride concentrations (Table 1), chloride condensation was suggested by evapotranspiration effects at the recharged zone in even the central GAB. Therefore, we chose 20 mg/L as the initial chloride concentration.

In the western GAB the chloride concentration is higher than in the central GAB. We measured the lowest chloride concentration of 82 mg/L in the recharge zone of the western GAB. Lehmann et al. [10] reported 119 mg/L at Duck Hole, and Torgersen et al. [6] used 300 mg/L as their initial chloride concentration. Because Love et al. [9] suggested that high chloride concentrations reflect condensation of fallout-deposited chloride infiltrating the thick unsaturated soil zone as a result of intense evapotranspiration, we chose 80 mg/L as the initial chloride concentration for path D in the western GAB. Our stable isotope data are also consistent with this choice.

In our measurements of the $^{36}\text{Cl}/\text{Cl}$ ratio, the highest values were $164.6 \pm 8.7 \times 10^{-15}$ at location 40 in the recharge zone in the central GAB and $136.5 \pm 8.7 \times 10^{-15}$ at location 57 in the western GAB. In the

central GAB, Bentley et al. [5] and Torgersen et al. [6] used values of 110×10^{-15} and 200×10^{-15} , respectively, as the initial cosmogenic ratio. In the western GAB, Love et al. [9] and Lehmann et al. [11] both used 125×10^{-15} as the initial cosmogenic ratio. We selected 200×10^{-15} for the central GAB, accepting the value chosen by Torgersen et al. [6], considering that we measured the highest value, $179.4 \pm 9.3 \times 10^{-15}$, at the Coonamble Embayment in the southern part of the central GAB [22]. We chose 150×10^{-15} for the western GAB considering that the observed highest value, $136.5 \pm 10 \times 10^{-15}$, in the western GAB exceeded the values chosen by Love et al. [9] and Lehmann et al. [11].

We estimated average secular equilibrium ratios for $^{36}\text{Cl}/\text{Cl}$ of $10.4 \pm 0.9 \times 10^{-15}$ for the Hooray Sandstone in the central GAB and $7.17 \pm 3.38 \times 10^{-15}$ for the Algebuckina Sandstone in the western GAB, using the methods of Feige et al. [23] and Andrews et al. [24] for U, Th, and light elements in the aquifer rocks (Table 3). Both ratios are slightly higher than the values of $9 \pm 3 \times 10^{-15}$ for the Hooray Sandstone in the central GAB reported by Bentley et al. [5] and 6×10^{-15} for the sandstone in the western GAB reported by Lehmann et al. [11]. The measured $^{36}\text{Cl}/\text{Cl}$ ratio was generally lower than 10×10^{-15} near Lake Eyre in the discharge zone. The lowest ratio we measured was $6.3 \pm 2.1 \times 10^{-15}$ at sampling site 47, which lies in overlapping discharge zones from both the central and western GAB. In this study, we took 6×10^{-15} as the secular equilibrium ratio for the purpose of calibration in both the central and western GAB.

3.4 Estimation of groundwater velocity calibrated by the $^{36}\text{Cl}/\text{Cl}$ ratio for groundwater dating

Infiltrated rainwater in the recharge zone contains atmospheric ^{36}Cl produced by cosmic rays that is not replenished once the rainwater reaches the water table and becomes isolated from atmospheric air. Cosmogenic ^{36}Cl formed by cosmic ray spallation of ^{39}K and ^{40}Ca in surface rock and soil may leach into this water, but the rate is negligible compared to the atmospheric source [25]. Thus, the number of ^{36}Cl atoms decreases with time along the flow path of groundwater moving from the recharge zone of a confined aquifer. Ultimately ^{36}Cl reaches a secular equilibrium level as its decay is balanced by geogenic ^{36}Cl produced from the reaction of (α, n) , which depends on the concentration of uranium and thorium, and the composition of light elements in the aquifer rocks. According to Phillips et al. [26],

the number of ^{36}Cl atoms can be expressed using the elapsed time T for the groundwater residence time as follows:

$$^{36}\text{Cl} = Cl_0 \cdot R_0 \cdot \exp(-\lambda \cdot T) + Cl_0 \cdot R_{eq} \cdot (1 - \exp(-\lambda \cdot T)) + R_{eq} \cdot (Cl(T) - Cl_0) \quad (1)$$

where $Cl(T)$ is the total chlorine concentration in groundwater at time T ; Cl_0 and R_0 are the initial value of the chlorine concentration and the initial $^{36}\text{Cl}/\text{Cl}$ ratio, respectively, in rainwater infiltrated in the recharge zone; R_{eq} is the secular equilibrium $^{36}\text{Cl}/\text{Cl}$ ratio in the aquifer and aquitard; and λ is the decay constant of ^{36}Cl ($2.31 \times 10^{-6} \text{ y}^{-1}$).

We can rewrite eq (1) as follows:

$$^{36}\text{Cl} = Cl_0 \cdot (R_0 - R_{eq}) \cdot \exp(-\lambda \cdot T) + R_{eq} \cdot Cl(T) \quad (2)$$

Using the subscript m to signify measured values and assuming $Cl(T) = Cl_m$ and $^{36}\text{Cl} = R_m \cdot Cl_m$, we can rewrite eq (2) as follows:

$$(R_m - R_{eq}) \cdot Cl_m = Cl_0 \cdot (R_0 - R_{eq}) \cdot \exp(-\lambda \cdot T) \quad (3)$$

$$\left(\frac{R_m - R_{eq}}{R_0 - R_{eq}} \right) \cdot \left(\frac{Cl_m}{Cl_0} \right) = \exp(-\lambda \cdot T) \quad (4)$$

We can rewrite eq (4) to solve for T as follows:

$$T = -\frac{1}{\lambda} \cdot \ln \left(\left(\frac{R_m - R_{eq}}{R_0 - R_{eq}} \right) \cdot \left(\frac{Cl_m}{Cl_0} \right) \right) \quad (5)$$

Equation (5) is the same one derived by Bentley et al. [5] and used by Torgersen et al. [6] in their GAB groundwater ^{36}Cl dating studies.

We can estimate elapsed time T from the groundwater flow velocity and position on the flow path. If we assume that groundwater flows with a constant velocity V from the recharge zone to the discharge point (sampling water-bore) along the flow path, we can derive the elapsed time as $T = L/V$, where L is the distance along the selected flow paths.

We can then rewrite eq (5) as

$$\frac{L}{V} = -\frac{1}{\lambda} \cdot \ln \left(\left(\frac{R_m - R_{eq}}{R_0 - R_{eq}} \right) \cdot \left(\frac{Cl_m}{Cl_0} \right) \right) \quad (6)$$

When we plot the data set of L vs. $\ln\left(\frac{R_m - R_{eq}}{R_0 - R_{eq}}\right) \cdot \left(\frac{Cl_m}{Cl_0}\right)$, we can estimate a constant velocity

V from the slope of the resulting line and then derive the residence time on the flow path from the distance along the flow path. Using eq (6), we extrapolated groundwater velocity V by correlating parameters of $^{36}\text{Cl}/\text{Cl}$ ratio and Cl concentration and flow distance L along the flow lines to the sampling water-bore, listed in Table 1.

We fitted eq. (6) to all plots in Fig. 7. The estimated slopes were -0.01742 ± 0.00238 ($r^2 = 0.828$) for path A, -0.0089 ± 0.0021 ($r^2 = 0.679$) for path C, and -0.00533 ± 0.00172 ($r^2 = 0.518$) for path D. The extrapolated groundwater velocities were 0.133 ± 0.018 m/y for path A, 0.260 ± 0.061 m/y for path C, and 0.433 ± 0.140 m/y for path D. Paths A, C, and D have a relatively high correlation between the $^{36}\text{Cl}/\text{Cl}$ ratio and L . But their velocities are smaller than the 0.67 m/y for the central basin and the 0.65 m/y for the western basin evaluated by Bethke et al. [8] from linear regression to the data of Torgersen et al. [6] through the J aquifer in the GAB. The differences in velocity were caused largely by differences in the selected flow paths.

We extrapolated groundwater velocities on the flow paths that were mainly constrained by cosmogenic ^{36}Cl dating. From these velocities and the flow distances, we estimated the longest residence time, 1.06×10^6 y, at the discharge area around Lake Eyre for path D. It is comparable to the estimate by Radke et al. [18] of $(1-2.2) \times 10^6$ y and the residence time greater than 10^6 y simulated in the groundwater flow analyses of the GAB by Bethke et al. [3,8].

3.5 Isotopic characteristics of ^4He dissolved in groundwater and correlation between ^4He concentration and distance from the recharge zone

Dissolved He concentration increases with distance from the recharge areas as the isotopic ratio of $^3\text{He}/^4\text{He}$ decreases. ^4He concentrations increase from the air saturation level of 10^{-8} ccSTP/g to more than 10^{-4} ccSTP/g, whereas the $^3\text{He}/^4\text{He}$ ratio falls from 1.5×10^{-6} to $(2-8) \times 10^{-8}$. The $^3\text{He}/^4\text{He}$ ratios for the Hooray Sandstone and Algebuckina Sandstone aquifers and for the mudstones of the aquitards confining these aquifers have been estimated at $6.7 \pm 3.5 \times 10^{-9}$ for the aquifers and $1.06 \pm 0.61 \times 10^{-8}$

for the aquitards by analytical methods [27] using the U, Th, and Li contents in the rocks (Table 3). This indicates that the crustal ^4He component, which mainly consists of radiogenic ^4He , has been accumulating in the groundwater during its flow in the confined aquifer.

Bethke and Johnson [3] noted that the ^4He concentration of groundwater in an aquifer is expressed by linear accumulation if the ^4He flux across basal boundary is a large and poorly constrained source. Torgersen and Ivey (eq. (7) in [28]) also described the dissolved ^4He concentration in confined aquifers in the GAB using a two-dimensional advection and dispersion model with uniform in situ ^4He production and a uniform ^4He flux at the bottom. They mentioned that ^4He accumulation over short distances was controlled by in situ production, and that over long distances was controlled by degassing flux. Here, we tested the correlation between dissolved ^4He concentration and distance from the recharge zone on each selected flow path.

We plotted data of flow distance (Table 1) and ^4He concentration on flow paths A, C, and D in Fig. 8. Each flow path is relatively acceptable for the linear correlation between ^4He concentration and distance from the recharge zone; $^4\text{He} = 10.20 \pm 2.76 \times 10^{-8} \times L + 6.85 \pm 3.92 \times 10^{-6}$ ($r^2 = 0.533$) for path A, $^4\text{He} = 21.40 \pm 5.60 \times 10^{-8} \times L - 2.44 \pm 6.14 \times 10^{-6}$ ($r^2 = 0.630$) for path C, and $^4\text{He} = 24.50 \pm 7.02 \times 10^{-8} \times L - 1.88 \pm 1.81 \times 10^{-5}$, ($r^2 = 0.582$) for path D. Therefore, we can at least approximate the ^4He concentration expressed by the linear equation $^4\text{He} = \alpha \cdot L + \beta$, where α and β are constants. As distance can be replaced by elapsed time, ^4He concentration can be rewritten as $^4\text{He} = \alpha \cdot T + \beta$. This may suggest that each flow path has a short length and a relatively uniform aquifer thickness. In other words, in Torgersen's eq. (7) [28], if an aquifer thickness h is constant at H and groundwater velocity is constant at U , ^4He concentration can be rewritten as

$$P \cdot \left(\frac{x}{U} \right) + \frac{F'}{H} \cdot \left(\frac{x}{U} \right) + \left(\frac{HF'}{k} \right) \cdot \left(\frac{1}{3} \right) + \text{diffusion term} \quad (7)$$

The equation is linearly controlled by the constant in situ He production P , the constant diffusion coefficients k , and the constant degassing flux F' , because the third term is constant and the fourth diffusion term decreases with increasing distance (time) [28].

Finally, we concluded that ^4He concentration can be roughly estimated by the linear correlation with

distance in our selected flow paths. As distance is equivalent to elapsed time T , if groundwater flow velocity is constant, the ^4He concentration can be expressed by $^4\text{He}_{\text{ex}} = \alpha \cdot T$ using the He accumulation rate α (ccSTP/gy $^{-1}$).

3.6 Estimation of ^4He accumulation rate calibrated by $^{36}\text{Cl}/\text{Cl}$ ratio for groundwater dating

The elapsed time (residence time) is described as $T = ^4\text{He}_{\text{ex}}/\alpha$ from the dissolved helium concentration $^4\text{He}_{\text{ex}}$ in a short flow path. This method takes the excess ^4He concentration to correspond to time under the assumption that losses from mixing, degassing, dispersion, and diffusion of ^4He are negligible under a steady state condition on flow paths A, C, and D. In the same manner as in section 3.4, we can rewrite eq (5) using $^4\text{He}_{\text{ex}}$ and α :

$$\frac{^4\text{He}_{\text{ex}}}{\alpha} = -\frac{1}{\lambda} \cdot \ln \left(\left(\frac{R_m - R_{eq}}{R_0 - R_{eq}} \right) \cdot \left(\frac{Cl_m}{Cl_0} \right) \right) \quad (8)$$

Analogously, we can derive α from a plot of $^4\text{He}_{\text{ex}}$ against $\ln \left(\left(\frac{R_m - R_{eq}}{R_0 - R_{eq}} \right) \cdot \left(\frac{Cl_m}{Cl_0} \right) \right)$, then use it to estimate residence times, even for extremely old waters in which ^{36}Cl is at secular equilibrium.

We estimated the accumulation rate for excess ^4He flow paths A, C, and D by fitting eq (8) to the data set of excess ^4He and the parameters of $\ln \left(\left(\frac{R_m - R_{eq}}{R_0 - R_{eq}} \right) \cdot \left(\frac{Cl_m}{Cl_0} \right) \right)$. The analytical results

for the flow paths are shown in Fig. 9.

We estimated He accumulation rates for the selected three groundwater flow paths: $1.85 \pm 0.31 \times 10^{-11}$ ccSTP/cm 3 ·y ($r^2 = 0.754$) for path A (central GAB), $7.01 \pm 1.87 \times 10^{-11}$ ccSTP/cm 3 ·y ($r^2 = 0.621$) for path C (central GAB), and $1.51 \pm 0.63 \times 10^{-10}$ ccSTP/cm 3 ·y ($r^2 = 0.485$) for path D, in which some samples (No. 48 and 49) were excluded owing to mixing (in the western GAB). In our estimations, paths A, C, and D showed a relatively strong correlation between excess ^4He concentration and ^{36}Cl age. The estimated accumulation rates, ranging from 1.85×10^{-11} to 1.51×10^{-10} ccSTP/cm 3 ·y, were well above the maximum in situ production rate of 6×10^{-13} ccSTP/cm 3 ·y (Table 3). Although each flow path has a significant external He component besides the in situ He production, path D has

accumulated the degassing He component more than paths A and C. The He accumulation rate is greatly different on each path.

Our estimates of the ^4He accumulation rate in the central GAB are approximately 2 to 15 times lower than the rate of $2.91 \times 10^{-10} \text{ ccSTP/cm}^3 \cdot \text{y}$ estimated by Torgersen and Clarke [4]. This probably reflects differences in the regional groundwater flow paths chosen and the water-bores sampled. Furthermore, the dissolved ^4He measurements varied greatly owing to degassing from groundwater samples, all of which displayed degassed bubbles at the mouth of their wells. Although the dissolved ^4He concentration has much uncertainty, the ^4He accumulation rate is probably well constrained on the selected flow paths by the ^{36}Cl reference age. Lehmann et al. [11] estimated the He accumulation rate in the western GAB as $(0.2\text{--}1.9) \times 10^{-10} \text{ ccSTP/cm}^3 \cdot \text{y}$ using ^{81}Kr ages. Our estimate of $1.51 \pm 0.63 \times 10^{-10} \text{ ccSTP/cm}^3 \cdot \text{y}$ for flow path D is consistent with Lehmann's estimate. The estimated residence time was approximately $7 \times 10^5 \text{ y}$ from the ^4He accumulation rate near Lake Eyre. Both proposed estimations are compatible with a 30% error.

Consequently, we can determine groundwater residence times beyond the equilibrium time of ^{36}Cl on the basis of excess ^4He concentrations and ^4He accumulation rates calibrated with ^{36}Cl ages. However, dissolved ^4He concentrations have high uncertainties owing to ^4He fluxes from outside the aquifer and degassing during sampling at water-bores in the discharge area.

4. Conclusions

- (1) We judged for each groundwater flow path whether the decreasing ratio of $^{36}\text{Cl}/\text{Cl}$ was controlled by decay of cosmogenic ^{36}Cl by comparison of the $^{36}\text{Cl}/\text{Cl}$ ratio together with $1/\text{Cl}$. Groundwater flow path E exhibited a strong evapotranspiration effect in the recharge area. Paths B and F displayed effects of mixing, with ^{36}Cl decreasing from dissolution from aquifer rock and diffusion from adjoining aquitards. On the other hand, ratios of $^{36}\text{Cl}/\text{Cl}$ were largely controlled by cosmogenic decay in paths A, C, and D (except in the discharge area of path D). We selected flow paths A, C, and D for estimation of groundwater dating. These three paths have relatively good linear correlation between dissolved ^4He concentration and flow distance from the recharge area.

On these paths, ^4He concentration can be approximated by a linear relation with a constant accumulation rate and elapsed time.

- (2) We estimated groundwater flow velocity for the regional groundwater flow paths based on ^{36}Cl -dated water samples and their distance from the recharge area along the flow paths. The extrapolated velocities were 0.133 ± 0.018 m/y for path A, 0.260 ± 0.061 m/y for path C, and 0.433 ± 0.140 m/y for path D. The estimated residence time of 1.06×10^6 y at the discharge area around Lake Eyre for path D is comparable to the estimate of $(1\text{--}2.2) \times 10^6$ y in previous studies.
- (3) We estimated ^4He accumulation rates for the selected flow paths: $1.85 \pm 0.31 \times 10^{-11}$ ccSTP/cm 3 ·y for path A (central GAB), $7.01 \pm 1.87 \times 10^{-11}$ ccSTP/cm 3 ·y for path C (central GAB), and $1.51 \pm 0.63 \times 10^{-10}$ ccSTP/cm 3 ·y for path D (western GAB). The estimated accumulation rates, ranging from 1.85×10^{-11} to 1.51×10^{-10} ccSTP/cm 3 ·y, were 2 to 15 times lower than rates reported in previous studies. However, our estimated rate of 1.51×10^{-10} ccSTP/cm 3 ·y $^{-1}$ in the western GAB is compatible with previous estimates of $(0.2\text{--}1.9) \times 10^{-10}$ ccSTP/cm 3 ·y $^{-1}$ based on ^{81}Kr ages. The estimated residence time was approximately 7×10^5 y from the ^4He accumulation rate near Lake Eyre.

Finally, we can extend this method to estimate residence times after reaching secular equilibrium for ^{36}Cl , if the groundwater velocity and ^4He accumulation rate are constant.

Acknowledgments

We thank L. K. Fifield (Australian National University), R. G. Cresswell (Commonwealth Scientific and Industrial Research Organisation), and M. Suter and H. A. Synal (Swiss Federal Institute of Technology) for measuring ^{36}Cl in groundwater.

We also thank two anonymous reviewers for their critical and constructive comments on the manuscript.

References

- [1] Davis S. N., Bentley H. W., 1982, Dating groundwater A short review, in: Currie L. A. (ed) Nuclear and Chemical Dating Techniques- Interpreting the Environmental Record, ACS Symposium Series 176, America Chemical Society, Washington, D. C., pp. 186-222.
- [2] Cook P., Herczeg A. L. (eds), 2000, Environmental tracers in subsurface hydrology, Kluwer Academic Publishers, Boston/Dordrecht/London, pp.529.
- [3] Bethke C. M. and Johnson T. M., 2008, Groundwater age and groundwater age dating, *Annu. Rev. Earth Planet. Sci.*, 36, 121-152.
- [4] Torgersen T., Clarke W. B., 1985, Helium accumulation in groundwater, I: An evaluation of sources and the continental flux of crustal ^4He in the Great Artesian Basin, Australia. *Geochim. Cosmochim. Acta.*, 49, 1211-1218.
- [5] Bentley H. W., Phillips F. M., Davis S. N., Habermehl M. A., Airey P. L., Calf G. E., Elmore D., Gove H. E. and Torgersen T., 1986, Chlorine 36 dating of very old groundwater 1. The Great Artesian Basin, Australia. *Water Resour. Res.* 22, 1991-2001.
- [6] Torgersen T., Habermehl M. A., Phillips F. M., Elmore D., Kubik P., Jones B. G., Hemmick T. and Gove H. E., 1991, Chlorine-36 dating of very old groundwater 3. Further studies in the Great Artesian Basin, Australia. *Water Resour. Res.* 27, 3201-3213.
- [7] Zhao X., Fritzel T. L. B., Quinodoz, Bethke C. M. and Torgersen T., 1998, Controls on the distribution and isotopic composition of helium in deep groundwater flows, *Geology*, 26, 291-294.
- [8] Bethke M. C., Zhao X., Torgersen T., 1999, Groundwater flow and the ^4He distribution in the Great Artesian Basin of Australia. *J. Geophys. Res.*, 104 NO. B6, 12999-13011.
- [9] Love A. J., Herczeg A. L., Sampson L., Cresswell R. G. and Fifield L. K., 2000, Sources of chloride and implications for ^{36}Cl dating of old groundwater, southwestern Great Artesian Basin, Australia. *Water Resour. Res.* 36, 1561-1574.
- [10] Park J., Bethke C. M., Torgersen T., Johnson T. M., 2002, Transport modeling applied to the interpretation of groundwater ^{36}Cl age, *Wat. Resour. Res.*, 38, NO. 5, 10.1029/2001 WR000399.
- [11] Lehmann B. E., Love A., Purtschert R., Collon P., Loosli H. H., Kutschera W., Beyerle U., Aeschbach-Hertig W., Kipfer R., Frape S. K., Herczeg A., Moran J., Tolstikhin N.I. and Gröning M., 2003, A comparison of groundwater dating with ^{81}Kr , ^{36}Cl and ^4He in four wells of the Great Artesian Basin, Australia. *Earth Planet. Sci. Lett.* 211, 237-250.
- [12] Hasegawa T., 2007, Study on verification of groundwater flow analytical models using the groundwater dating result, Th. Doct. Graduate School of Environmental Science, Okayama University.
- [13] Hasegawa T., Mahara Y., Nakata K., Habermehl M. A., 2008, Verification of ^4He and ^{36}Cl dating for very old groundwater in Great Artesian Basin, Australia, Proceedings of 36th IAH Congress, Integrating Groundwater Science and Human Well-being, October 2008 Toyama, Japan.
- [14] Habermehl M. A., 1980, The Great Artesian Basin, Australia. *BMR Journal of Australian Geology & Geophysics* 5, 9-38.
- [15] Habermehl M. A., 2001, Hydrogeology and environmental geology of the Great Artesian Basin,

- Australia. in: Gostin V.A. (Ed.) Gondwana to Greenhouse - Australian Environmental Geoscience. Geological Society of Australia Inc., Special Publication, 21, 127-143, 344-346.
- [16] Habermehl M. A. and Lau J. E., 1997, Hydrogeology of the Great Artesian Basin (Map at scale 1:2 500 000), Australian Geological Survey Organisation, Canberra.
- [17] Welsh W. D., 2000, GABFLOW: A steady state groundwater flow model of Great Artesian Basin, *Report, Land & Water Sciences Division, Bureau of Rural Sciences, Canberra.*
- [18] Radke B.M., Ferguson J., Cresswell R.G., Ransley T.R. and Habermehl M.A., 2000, Hydrochemistry and implied hydrodynamics of the Cadna-owie - Hooray Aquifer, Great Artesian Basin, Australia. *Bureau of Rural Sciences, Canberra*, 229 pp.
- [19] Seidel G. E., 1980, Application of the GABHYD groundwater model of the Great Artesian Basin, Australia. *BMR Journal of Australian Geology & Geophysics*, 5, 39-45.
- [20] Mahara Y., Hasegawa T., Miyakawa K. and Ohta T., 2008, Correlation between dissolved ^4He concentration and ^{36}Cl in groundwater at Äspö, Sweden. *Appl. Geochem.* 23, 3305-3320.
- [21] Coplen T. B. and Hanshaw B. B., 1973, Ultrafiltration by a compacted clay membrane-I. Oxygen and hydrogen isotopic fractionation, *Geoch. Cosmochim. Acta*, 37, 2295-2310.
- [22] Mahara Y., Habermehl M. A., Miyakawa K., Shimada J. and Mizuochi Y., 2007, Can the 4He clock be calibrated by ^{36}Cl for groundwater dating?, *Nucl. Instr. and Meth. in Phys. Res. B* 259, 536-546.
- [23] Feige Y., Oltman B.G. and Kastner J., 1968, Production rates of neutrons in soils due to natural radioactivity. *J. Geophys. Res.* 73, 3135-3142.
- [24] Andrews J.N., Fontes J.-Ch., Michelot J.-L. and Elmore D., 1986, In-situ neutron flux, ^{36}Cl production and groundwater evolution in crystalline rocks at Stripa, Sweden. *Earth Planet. Sci. Lett.* 77, 49-58.
- [25] Phillips F. M., (2000), Chlorine-36. in: P.G. Cook, A.L. Herczeg (Eds.), *Environmental Tracers in Subsurface Hydrology*, Kluwer Academic, Dordrecht, pp.299-348.
- [26] Phillips F. M., Bentley H. W., Davis S. N., Elmore D. and Swanick B. G., 1986, Chlorine 36 dating of very old groundwater 2. Milk River aquifer, Alberta, Canada. *Water Resour. Res.* 22, 2003-2016.
- [27] Lehmann B. E. and Loosli H. H., 1991, Isotopes formed by underground production. in: Pearson F.J., Balderer W., Loosli H.H., Lehmann B. E., Matter A., Peters T., Schmassmann H. and Gautschi A. (Eds.), *Applied isotope hydrology - a case study in Northern Switzerland*. Elsevier Sci. Publ. Company Inc., New York, pp.239-265.
- [28] Torgersen T. and Ivey G. N., 1985, Helium accumulation in groundwater. II: A model for the accumulation of the crustal 4He degassing flux., *Geochim. Cosmochim. Acta*, 49, 2445-2452.

Figure captions

Fig. 1 Location of the Great Artesian Basin, Australian province names, sample locations (solid circles), and groundwater flow paths A through F. Red triangles mark locations where drill cores were sampled for physical and chemical analyses (see Table 3). Arrows show flow directions inferred from previous studies [14-18].

Fig. 2 Comparison between the distribution of $^{36}\text{Cl}/\text{Cl}$ ratio measured in GAB and the distribution of $^{36}\text{Cl}/\text{Cl}$ ratio obtained from three-dimensional transport analyses (after [12]). Open circle and number is location of well.

Fig. 3 Comparison between the distribution of ^4He concentration measured in GAB and the distribution of ^4He concentration obtained from three-dimensional transport analyses (after [12]). Open circle and number is location of well.

Fig. 4 Plot of δD and $\delta^{18}\text{O}$ ratios for artesian groundwater samples collected in the Great Artesian Basin and the correlation of two local meteoric water lines. The upper correlation line is $\delta\text{D} = 4.63 \pm 0.34 \times \delta^{18}\text{O} - 10.3 \pm 2.3$; $r^2 = 0.895$. The lower line is $\delta\text{D} = 5.69 \pm 0.28 \times \delta^{18}\text{O} - 11.06 \pm 2.1$; $r^2 = 0.949$. Solid square: flow path A, solid triangle: flow path B, open triangle: flow path C, solid circle: flow path D, open circle: flow path E, open star: flow path F.

Fig. 5 Correlation between $^{36}\text{Cl}/\text{Cl}$ ratios and inverse chloride concentration ($1/\text{Cl}$) along the six regional groundwater flow paths. Changes caused by various processes are illustrated. Mixing lines between cosmogenic ^{36}Cl atoms in meteoric water ($\text{Cl}: 1, 10, 100, 1000$; $\text{R}: 2 \times 10^{-13}$) and geogenic ^{36}Cl atoms at secular equilibrium in groundwater derived from aquitards ($\text{Cl}: 18\,000, \text{R}: 8 \times 10^{-15}$; $\text{Cl}: 30\,000, \text{R}: 20 \times 10^{-15}$) in GAB are shown.

Fig. 6 Correlation between $^{36}\text{Cl}/\text{Cl}$ ratio and dissolved ^4He concentration on groundwater flow paths A, C, and D.

Fig. 7 Correlation between $\ln\left(\left(\frac{R_m - R_{eq}}{R_0 - R_{eq}}\right) \cdot \left(\frac{Cl_m}{Cl_0}\right)\right)$ and distance L from the groundwater recharge area along flow paths A, C, and D.

Fig. 8 Correlation between excess dissolved ^4He concentration (ccSTP/g) and flow distance L (km) along flow paths A, C, and D.

Fig. 9 Correlation between $\ln\left(\left(\frac{R_m - R_{eq}}{R_0 - R_{eq}}\right) \cdot \left(\frac{Cl_m}{Cl_0}\right)\right)$ and excess dissolved ^4He concentration (ccSTP/g) for flow paths A, C, and D.

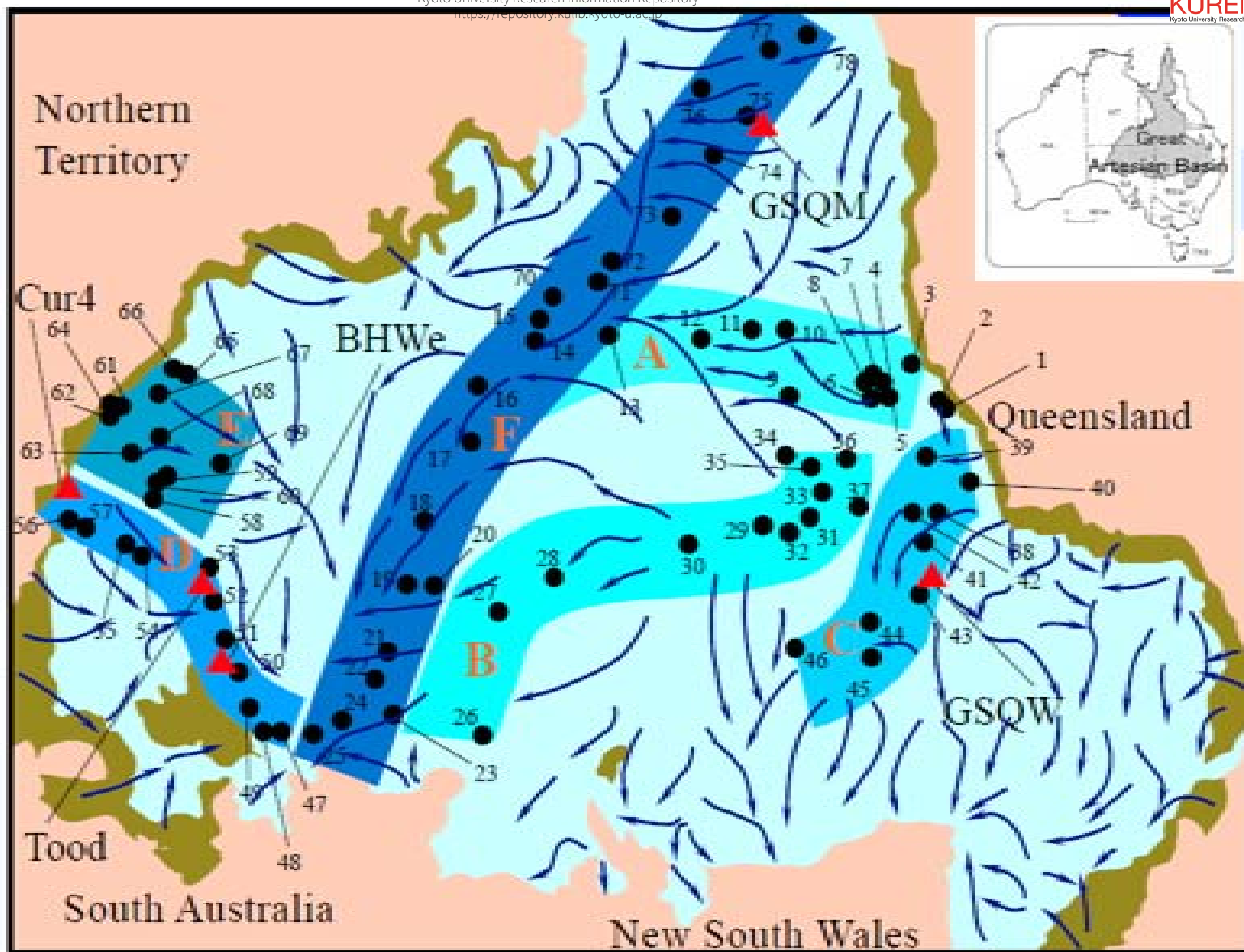
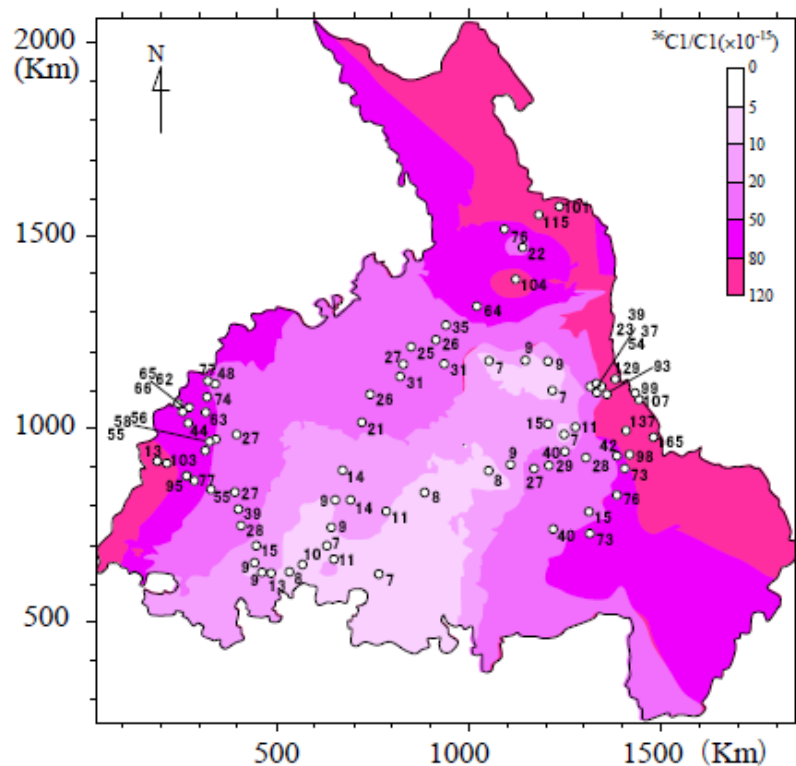


Fig-1

(Measurement of $^{36}\text{Cl}/\text{Cl}$)



(Analysis of $^{36}\text{Cl}/\text{Cl}$)

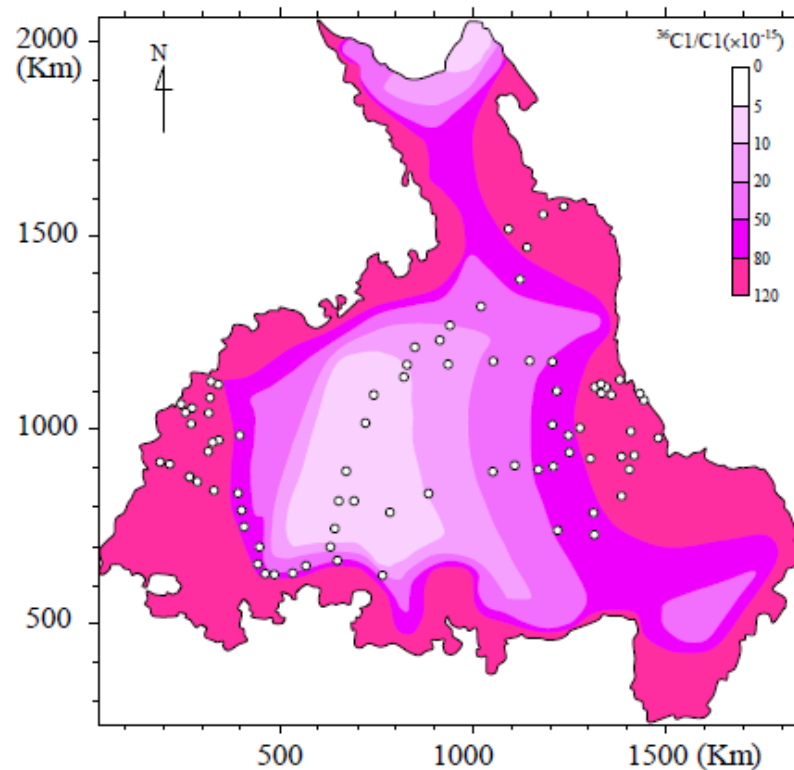
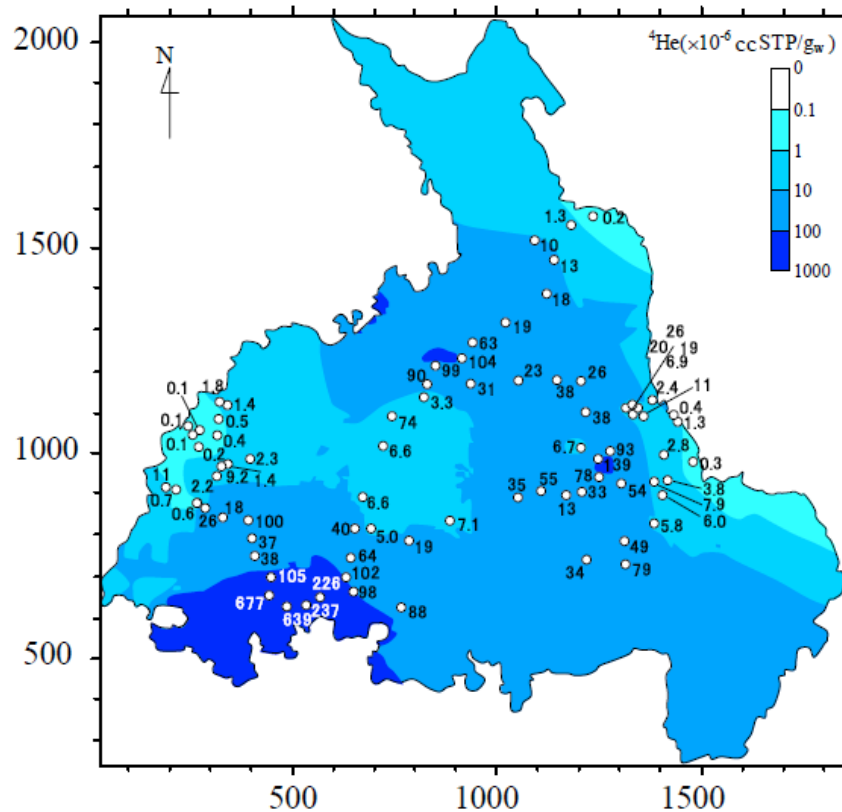


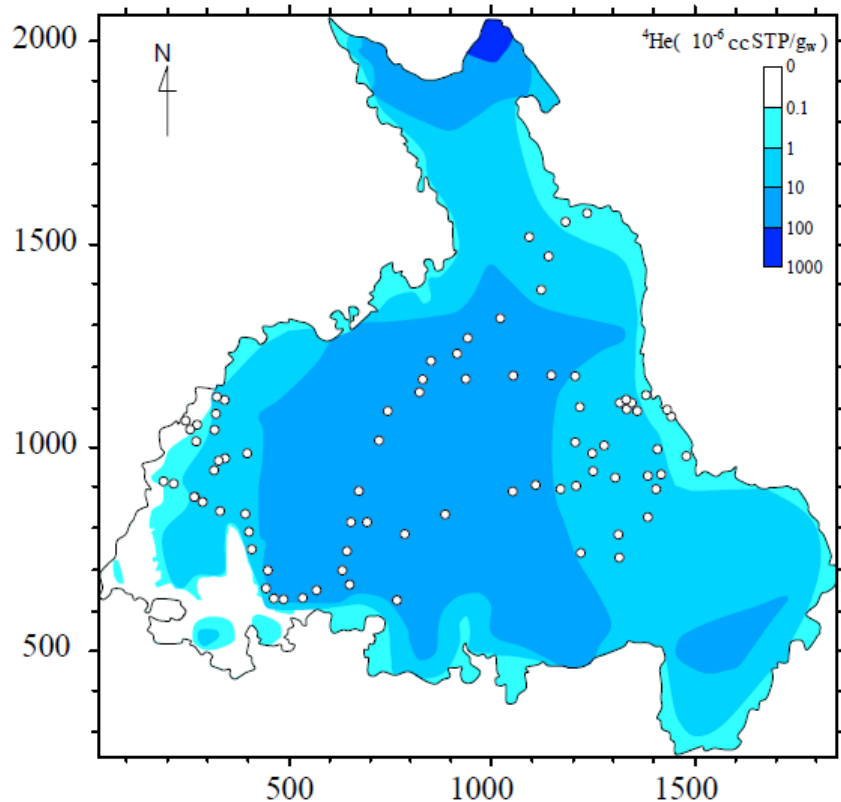
Fig- 2 200 1000 1200 (Km)



(Measurement of ^4He)



(Analysis ^4He)



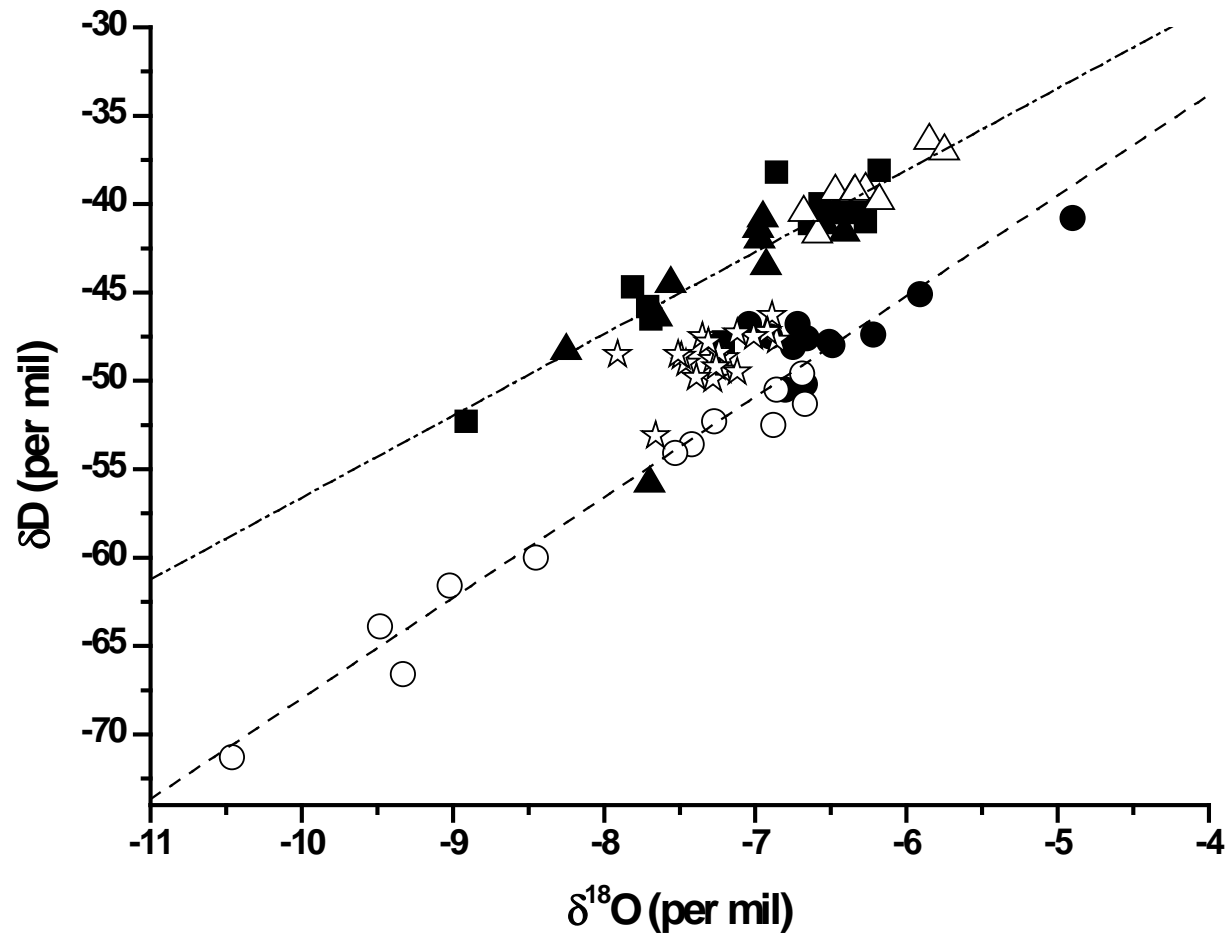


Fig-4

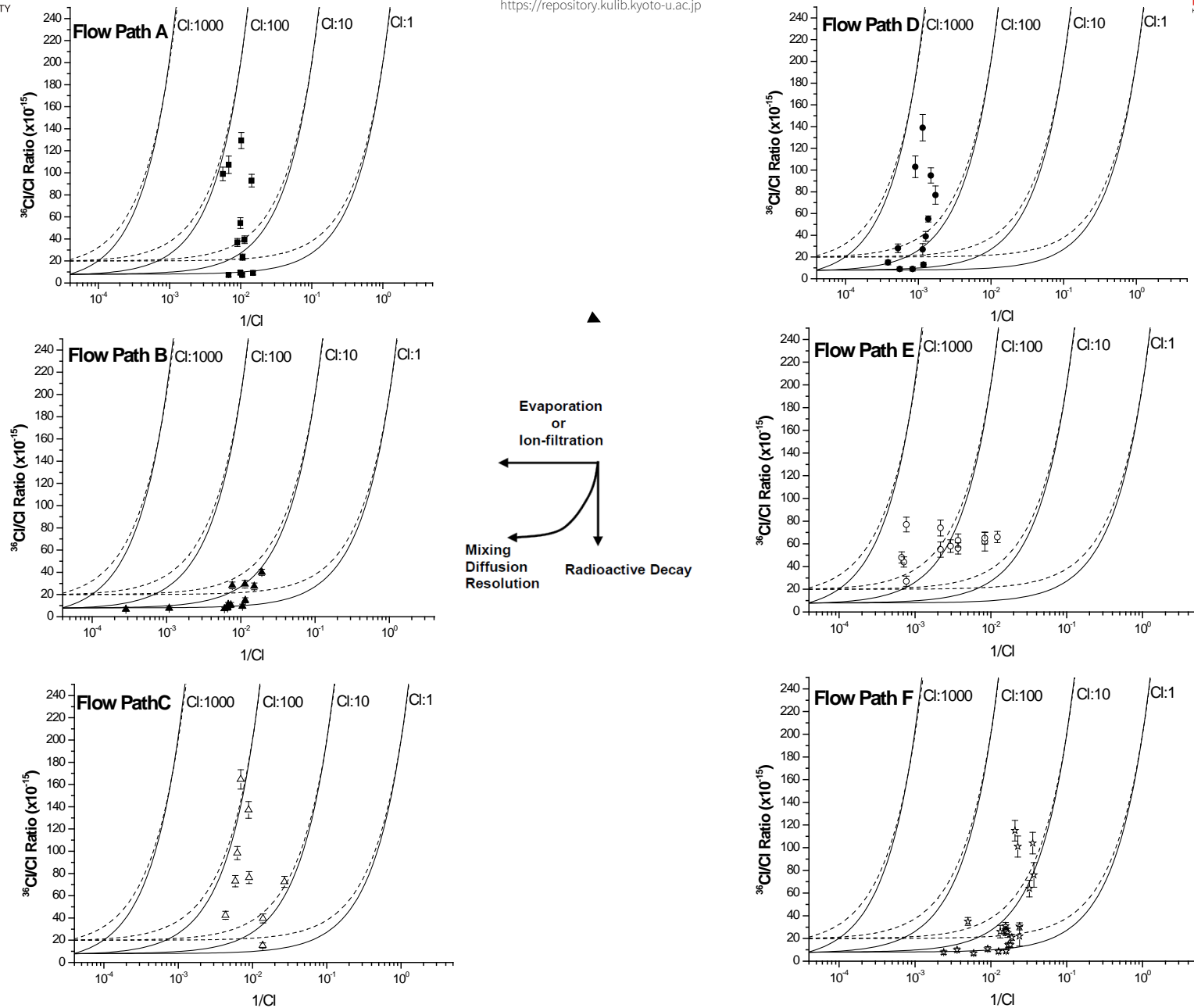


Fig-5

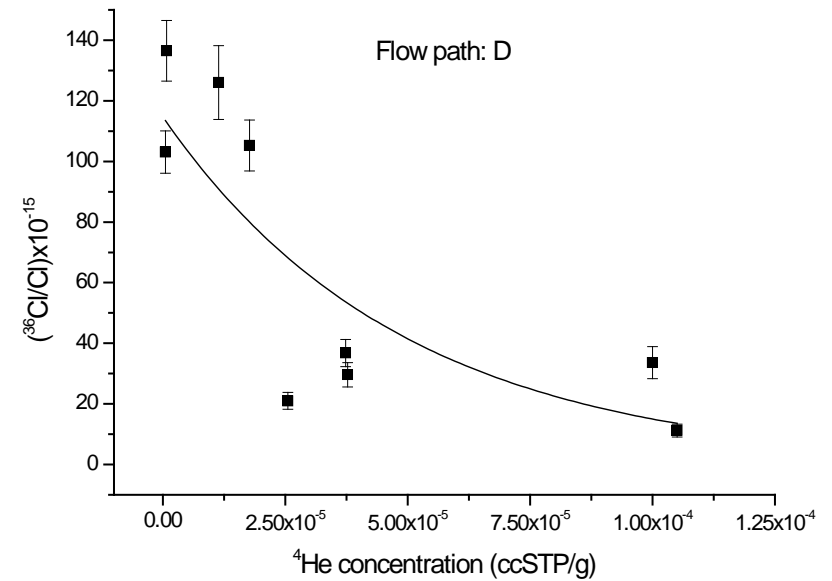
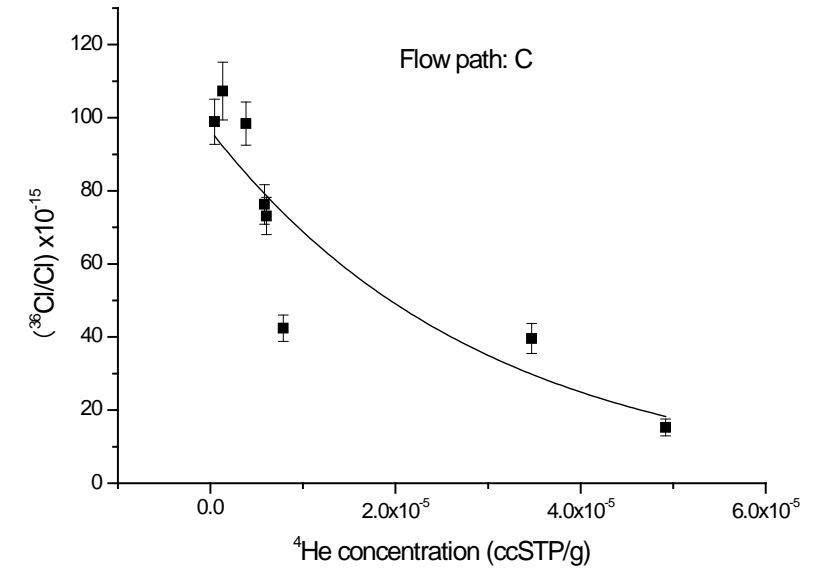
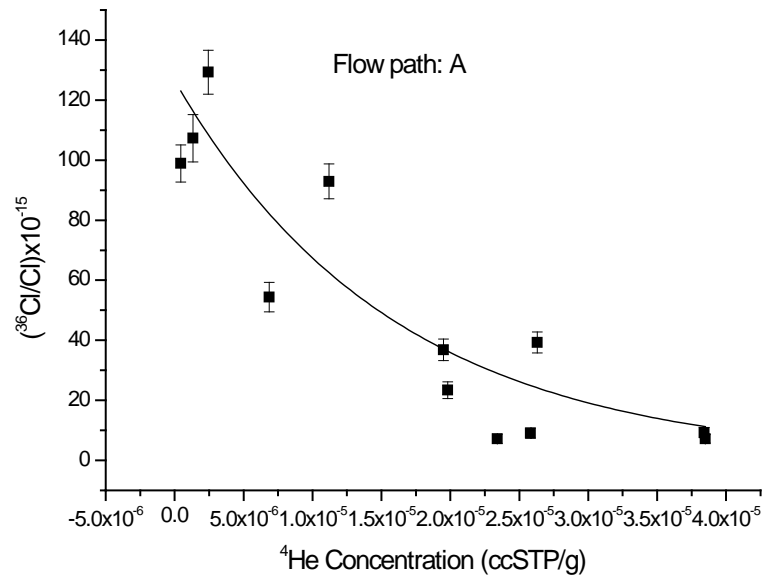


Fig-6

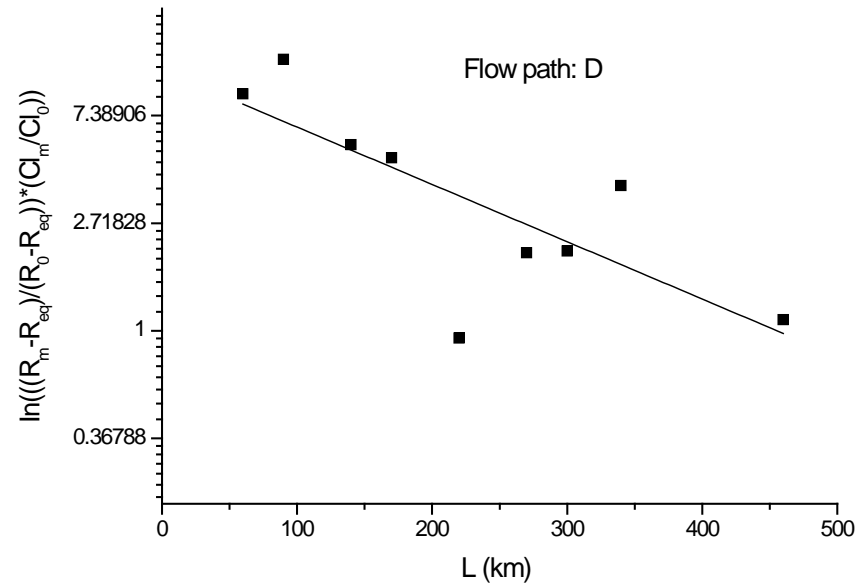
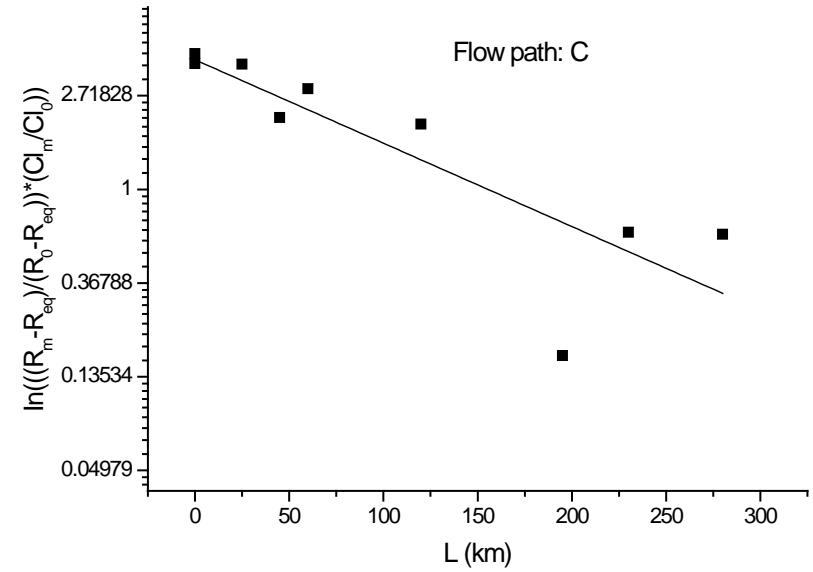
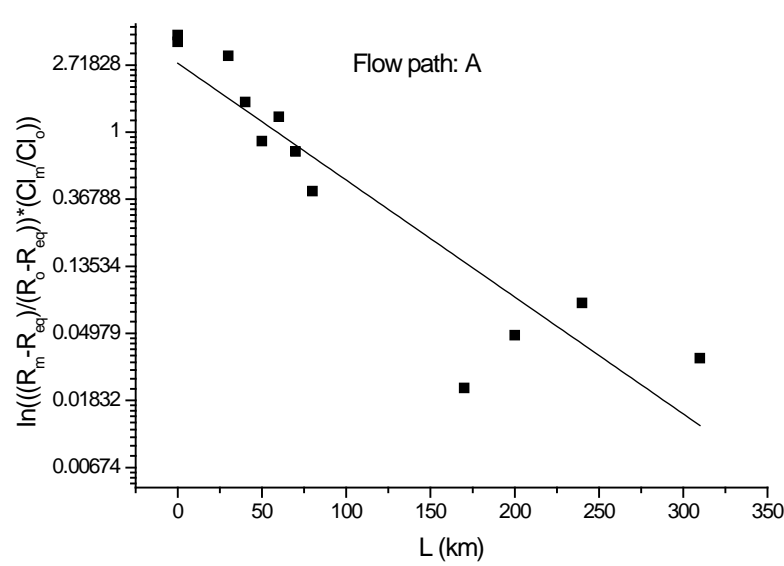


Fig-7

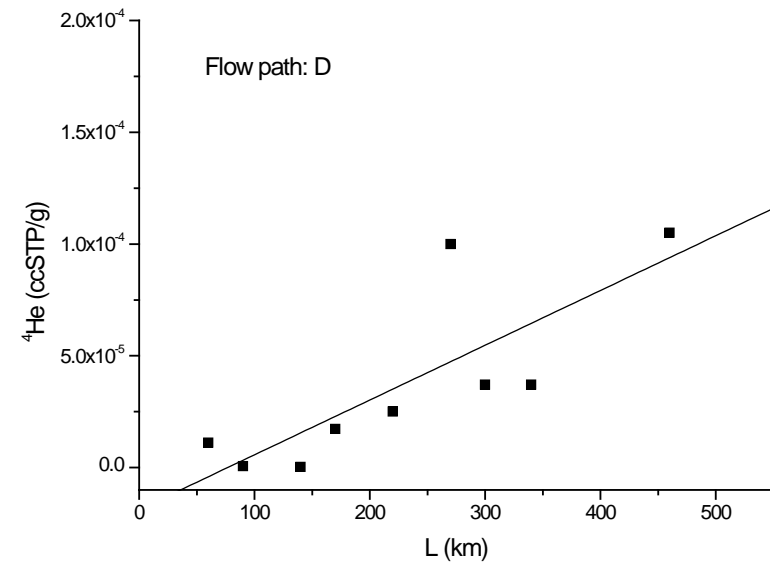
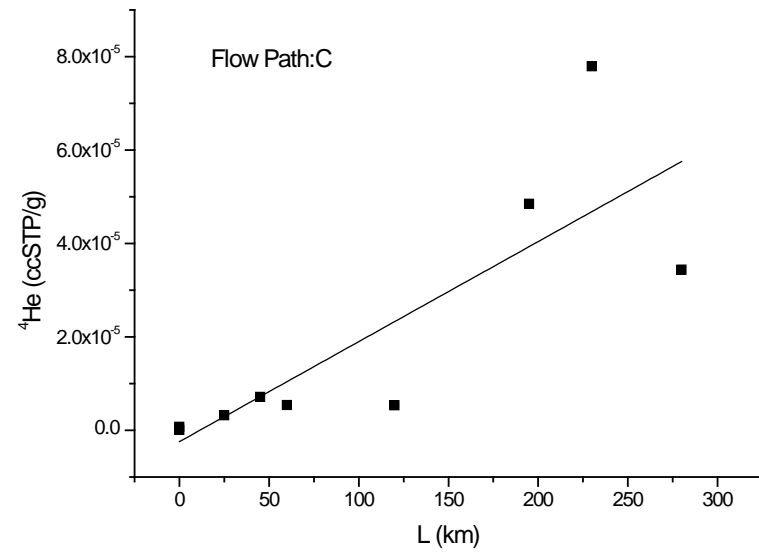
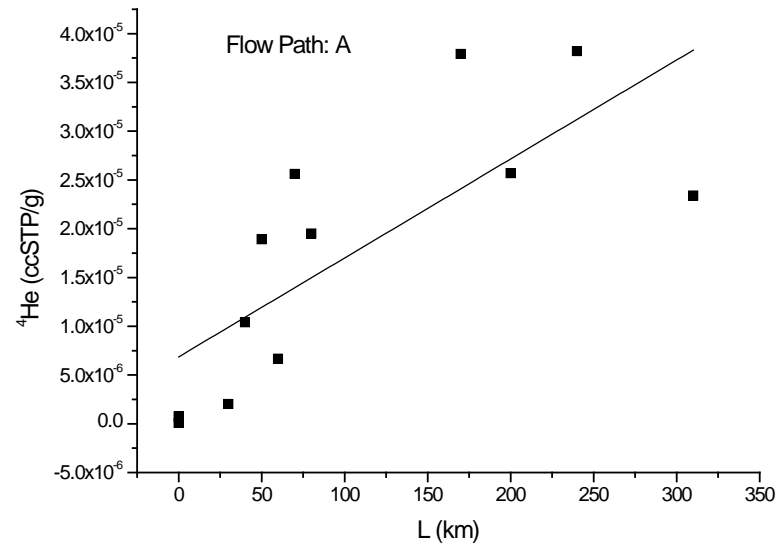


Fig-8

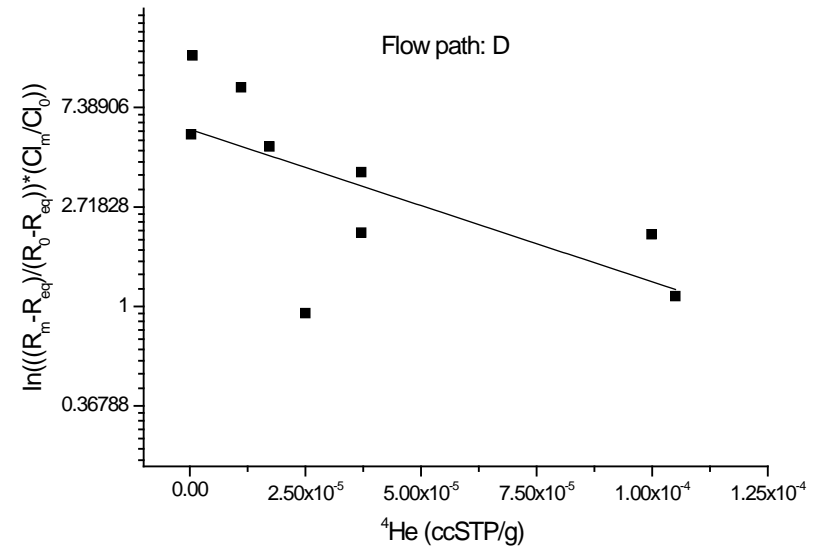
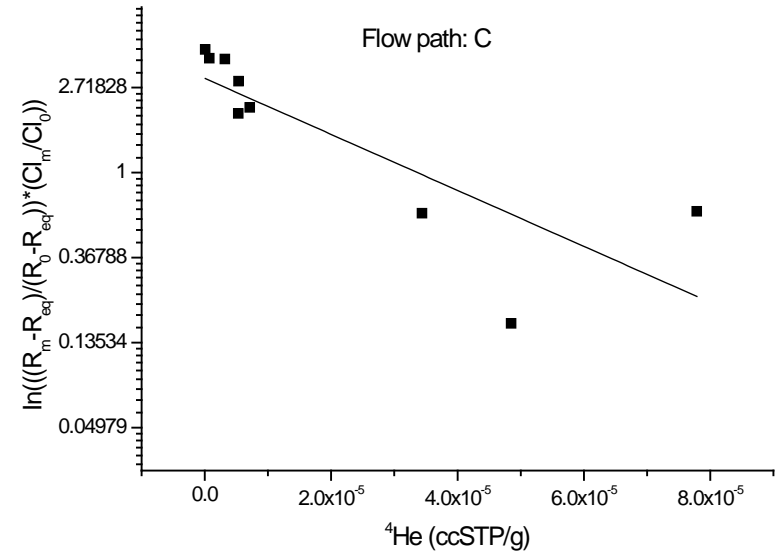
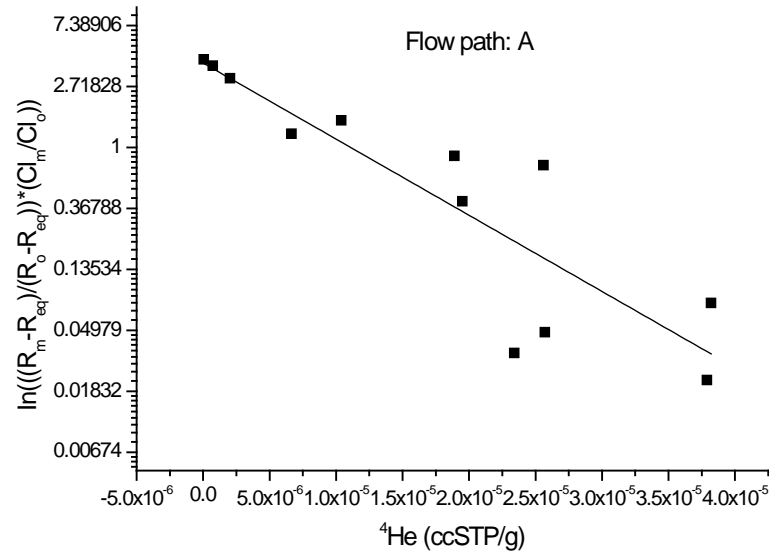


Fig- 9

Table-1 Data of all bores sampled for groundwater in the Great Artesian Basin, distance from the recharge area along regional groundwater flow paths, and in situ measured physical and hydrochemical data and chloride ion concentration.

Sample No.	Bore Number	Bore Nam	Flow (F) Pumped	Date (I Sampled)	Flow Path Distance fi Recharge(Flow Path Distance fi Recharge(Flow Path Distance fi Recharge(Flow Path Distance fi Recharge(Flow Path Distance fi Recharge(Flow Path Distance fi Recharge(Temp. °C	pH	Eh mV	EC S/m	DO mg/L	Cl mg/L
1	Q-12739	Tambo-5	P	2002/9/18							30.44	7.97	-151	0.0945	0.25	147
2	Q-10842	Wellwater	P	2002/9/18							29.24	6.77	-97	0.098	0.06	178
3	Q-4056	Northhamj	F	2002/9/19	30						42.76	8.74	-215	0.0738	0.23	98
4	Q-11445	Eastwood	F	2002/9/19	50						42.64	8.28	-264	0.146	0.16	111
5	Q-4064	North Avo	F	2002/9/20	40						50.47	8.57	-313	0.0717	0.39	70
6	Q-1551	Homebush	F	2002/9/20	60						65	8.15	-324	0.125	0.5	101
7	Q-378	Burra Bun	F	2002/9/21	70						59.6	8.01	-297	0.144	0.78	88
8	Q-4497	Athol	F	2002/9/21	80						65	7.8	-301	0.175	0.62	94
9	Q-1057	Gable End	F	2002/9/22	170						74.5	7.71	-333	0.219	0.58	95
10	Q-4270	Bonnie De	F	2002/9/22	200						87.3	7.48	-344	0.187	0.8	67
11	Q-1475	Whitewoo	F	2002/9/23	240						93.2	7.45	-365	0.21	0.12	101
12	Q-4782	Mutti Muti	F	2002/9/24	310						83.9	7.55	-358	0.281	1.17	148
13	Q-14486	Merabook	F	2002/9/25						450	63.7	8	-343	0.0897	0.68	42
14	Q-12312	Georgtina	F	2002/9/25						560	68.7	8.07	-271	0.089	2.25	64
15	Q-3822	Peppin-4/C	F	2002/9/26						550	59.5	7.62	-274	0.0849	0.77	64
16	Q-12177	Cacoory/C	F	2002/9/27						630	78.5	7.52	-332	0.0897	0.8	63
17	Q-14645	Birdsville	F	2002/9/27						680	98.5	7.75	-357	0.0903	0.83	53
18	S-6643-01	Goyder's I	F	2002/9/28						810	100.3	7.39	-345	0.106	0.67	59
19	S-6642-02	Mirra Mitt	F	2002/9/28						880	89.4	7.13	-331	0.199	0.53	63
20	S-6742-01	Kalladeina	F	2002/9/29						870	85.6	7.28	-326	0.125	0.82	55
21	S-6641-06	Mulka	F	2002/9/29						950	85.3	7.2	-330	0.134	0.84	79
22	S-6640-04	Cannawau	F	2002/9/30						1000	79.2	7.14	-313	0.161	1.06	169
23	S-6439-20	Muloorina	F	2002/9/30						1060	55.9	7.59	-240	0.216	1.27	279
24	S-6639-03	Cooryanin	F	2002/10/1						1020	55	7.42	-244	0.142	0.82	110
25	S-6439-09	Morris Cre	F	2002/10/1						1090	42.55	7.47	-235	0.246	0.31	418
26	S-6839-03	Montecolli	F	2002/10/5		770					46.3	7.51	-292	0.947	0.38	3510
27	S-6942-04	Gidgealpa	F	2002/10/6		700					93.9	7.71	-366	0.286	0.68	136
28	Q-16768	Innaminck	F	2002/10/7		590					45.3	7.01	-307	0.571	0.61	921
29	Q-358	Eromanga	F	2002/10/8		370					85.3	7.01	-322	0.256	0.62	95
30	Q-5092	Mt Margai	F	#####		430					64.6	6.82	-357	0.309	0.43	151
31	Q-390	Quilpie To	F	#####		280					75.5	7.92	-401	0.0982	0.57	88
32	Q-148	Whynot	F	#####		320					82.5	7.67	-373	0.1	0.45	66
33	Q-155	Winbin	F	#####		240					65.2	8.07	-385	0.0716	0.44	52
34	Q-3771	Milo Holdi	F	#####		250					95.5	7.51	-385	0.173	1.44	87
35	Q-305	Adavale T	F	#####		220					74.2	7.71	-343	0.197	0.72	166
36	Q-1184	Stannum	F	#####		190					50.3	7.53	-299	0.193	0.57	148
37	Q-1627	Boothella	F	#####		190					59.9	7.91	-334	0.156	0.6	130
38	Q-12615	Gowrie-4	F	#####			25				36.2	8.44	-314	0.107	0.2	160
39	Q-5287	Oakwood	F	#####		80					34.9	8.41	55	0.098	0.61	113
40	Q-6088	Burenda N	P	#####		40					32.7	7.16	-229	0.0971	0.22	144
41	Q-1996	Wallal	F	#####			60				40.2	8.23	-176	0.129	2.16	170
42	Q-2870	Combanni	F	#####			45				43.1	7.93	-302	0.166	0.3	231
43	Q-2049	Bonna Vis	F	#####			120				46.1	8.13	-264	0.091	0.92	111
44	Q-1338	Cocklarina	F	#####			195				47.1	7.95	-305	0.096	0.45	73
45	Q-2431	The Gap	F	#####			280				53.9	7.6	-285	0.0812	0.58	72
46	Q-2271	Kahmoo	F	#####			230				43.6	7.69	-267	0.0566	0.44	37
47	S-633916	Curdinmurk	F	2003/8/27						1120	31.38	7.23	-108	0.47	0.51	850
48	S-623904	Beresford	F	2003/8/28				510			32.28	6.75	-19	0.725	1.39	1800
49	S-624004	Armistice	F	2003/8/29				460			36.52	6.56	-49	0.987	0.77	2600
50	S-614153	Jerrys	F	2003/8/29				340			28.48	6.87	-209	0.764	0.36	1900
51	S-614205	Wood Duc	F	2003/8/30				300			38.01	7.08	-220	0.399	0.62	790
52	S-614204	Duckhole	F	2003/8/31				270			39.19	7.32	-208	0.405	0.79	870
53	S-594201	Oodnadatt	F	2003/8/31				220			40.54	7	-232	0.346	0.82	730
54	S-594317	Midway	F	2003/9/1				170			32.4	6.85	-174	0.331	0.4	580
55	S-584325	Marys We	F	2003/9/1				140			24.09	7.44	-108	0.389	3.68	670
56	S-574415	Lambina I	P	2003/9/2				60			31.6	6.71	97	0.35413	0.59	870
57	S-574404	Lambina S	P	2003/9/2				90			31.5	6.79	-110	0.47535	0.99	1100
58	S-594406	Junction	P	2003/9/3					140		44.8	6.83	-132	0.19729	1.5	460
59	S-604516	Dalhousie	P	2003/9/4					140		39.1	7.2	-98	0.13495	2.87	270
60	S-594575	Three O'C	F	2003/9/4					130		39.5	6.81	-147	0.13991	0.63	340
61	T-3230	New Crow	F	2003/9/5					30		27.5	6.95	86	0.06165	---	120
62	T-12945	Willoughby	F	2003/9/5					30		28.6	6.99	-44	0.05846	---	82
63	T-11587	Gidgea	P	2003/9/5					60		31.6	6.87	-152	0.38958	---	1400
64	T-17513	Finke Tow	P	2003/9/6					10		27.6	6.62	118	0.06947	---	120
65	T-2218	North	P	2003/9/7					40		37.3	6.9	-178	0.47764	---	1500
66	T-16954	Millenium	P	2003/9/7					30		31.3	6.6	-14	0.46809	---	1300
67	T-12959	Andado H	P	2003/9/8					50		35.2	6.96	-215	0.17409	---	460
68	T-17870	Mayfields	P	2003/9/8					70		35.8	6.92	-203	0.12672	---	270
69	S-614501	Purni-l	P	2003/9/9					170		70.5	6.73	-156	0.46178	---	1300
70	Q-2392	Ingledool	P	2003/9/13						560	58.5	7.23	-227	0.07194	0.32	60
71	Q-5100	Diamantin	F	2003/9/13						510	62.6	7.33	-231	0.0816	0.28	75
72	Q-10644	Mayne Pu	F	2003/9/13						460	65	7.53	-227	0.13941	0.31	200
73	Q-2237	Gidyea	F	2003/9/14						370	83.7	7.71	-320	0.08016	0.7	31
74	Q-407	Winton To	F	2003/9/15						260	80.9	7.28	-289	0.05019	2.79	28
75	Q-4375	Sesbania-ε	F	2003/9/15						180	62.1	6.9	-160	0.06431	1.3	42
76	Q-4455	Bora	F	2003/9/16						160	53.8	8.37	-271	0.06422	0.44	27
77	Q-15562	Kalboona	F	2003/9/16						80	36.1	8.24	-251	0.07936	0.09	48
78	Q-57	Fairlight	T	2003/9/17						30	31.7	6.55	-90	0.07671	0.34	44
79	S-623923	Big Bubbl	F	2003/8/28				540		---	---	---	---	---	---	1200

Q - Queensland S - South Australia T - Northern Territory

Temp. - Temperature Eh - Redox potential EC - Electrical conductivity DO - Dissolved Oxygen

Table 2. Chloride ion, ^{14}C , ^{36}Cl , dissolved He, and dissolved Ne concentrations in 79 groundwater samples collected in the Great Artesian Basin.

Sample	Ne	Chloride ic 3H	±error	^{14}C	±error	$^{36}\text{Cl}^*$	He	Ne (tot)
		Concentrat Bq/l	Bq/l	$\delta^{13}\text{C} \text{ ‰}$	$^{14}\text{CpmC} \text{ ‰}$	$^{36}\text{Cl/Cl} \times 10^{-15}$	$^3\text{He/4He}$	Excess ^4He
		(mg/L)		‰	%	$\times 10^{-15}$	(ccSTP/g)	(ccSTP/g)
1		147 N.D.		-18.8	2.9	0.1	0.2	7.36E-07
2		178 N.D.		-18.3	10.7	0.1	0.19	6.64E-08
3		98 N.D.		-17.9	3.4	0.1	0.12	2.03E-06
4		111 N.D.		-7.2	1.4	0.1	0.07	1.89E-05
5		70 N.D.		-16.6	3.3	0.1	0.07	1.04E-05
6		101 N.D.		-7.4	1.3	0.1	0.08	6.66E-06
7		88 N.D.		-5.7	1.3	0.1	0.05	2.56E-05
8		94 N.D.		-3.8	1.4	0.1	0.04	1.95E-05
9		95 N.D.		-2.2	1.3	0.1	0.02	3.79E-05
10		67 N.D.		-2.1	1.5	0.1	0.02	2.57E-05
11		101 N.D.		-2.2	1.6	0.1	0.03	3.82E-05
12		148 N.D.		-4	1.4	0.1	0.04	2.34E-05
13		42 N.D.		-9.8	1.7	0.1	0.02	3.04E-05
14		64 N.D.		-11.4	1.7	0.1	0.03	3.10E-06
15		64 N.D.		-12.2	1.7	0.1	0.03	8.98E-05
16		63 N.D.		-10.3	1.8	0.1	0.03	7.31E-05
17		53 N.D.		-9.9	1.6	0.1	0.02	6.40E-06
18		59 N.D.		-7.1	1.2	0.1	0.02	6.53E-06
19		63 N.D.		-5.9	1	0.1	0.02	4.00E-05
20		55 N.D.		-5	1.5	0.1	0.02	4.91E-06
21		79 N.D.		-5.5	1.3	0.1	0.02	6.36E-05
22		169 N.D.		-5.5	1.1	0.1	0.04	1.02E-04
23		279 N.D.			1.6	0.1	0.08	2.25E-04
24		110 N.D.		-5.1	1.1	0.1	0.11	9.76E-05
25		418 N.D.		-5.7	1.5	0.1	0.13	2.36E-04
26		3510 N.D.		-11.7	4.4	0.1	1.07	8.73E-05
27		136 N.D.		-0.7	1.6	0.1	0.05	1.89E-05
28		921 N.D.		-3.6	1.3	0.1	0.28	6.82E-06
29		95 N.D.		0.8	1.7	0.1	0.03	5.47E-05
30		151 N.D.		0	1.7	0.1	0.05	3.52E-05
31		88 N.D.		-6.6	2.1	0.1	0.05	3.19E-05
32		66 N.D.		-3.5	1.2	0.1	0.03	1.20E-05
33		52 N.D.		-9.6	2	0.1	0.02	7.78E-05
34		87 N.D.		-1.4	1.4	0.1	0.03	6.69E-06
35		166 N.D.		-3.9	1.7	0.1	0.04	1.37E-04
36		148 N.D.		-4.9	1.7	0.1	0.05	9.18E-05
37		130 N.D.		-3	1.3	0.1	0.07	5.27E-05
38		160 N.D.		-13.4	1.8	0.1	0.16	3.20E-06
39	0.05	0.02	-14.8	2.3	0.1	137.2	0.14	2.05E-06
40	0.12	0.02	-12	4.7	0.1	164.6	0.6	1.79E-06
41			-10	1.3	0.1	73.1	0.15	5.38E-06
42	0.05	0.02	-7.8	1.1	0.1	42.4	0.14	7.14E-06
43			-9.3	1.8	0.1	76.3	0.1	5.33E-06
44			-1.2	1.2	0.1	15.3	0.03	4.85E-05
45			-7.9	1.6	0.2	39.6	0.05	3.44E-05
46			-9.8	1.9	0.2	72.5	0.03	7.79E-05
47			-5.2	1.8	0.1	6.3	0.63	6.38E-04
48			-7.3	1.9	0.1	8.4	0.62	6.76E-04
49			-9.2	1	0.1	11.2	1.24	1.05E-04
50			-10.5	3.5	0.1	29.6	1.22	3.71E-05
51			-8.7	2.7	0.1	36.8	0.64	3.71E-05
52			-9.6	2.8	0.1	33.6	0.63	9.99E-05
53	0.05	0.02	-10.9	2.9	0.1	21	0.91	2.50E-05
54			-8.9	2.5	0.1	105.3	0.61	1.72E-05
55			-8.1	9.5	0.1	103.1	0.73	2.86E-07
56			-11	5.8	0.1	126	1.99	1.11E-05
57			-9.4	3.9	0.1	136.5	1.41	5.88E-07
58	0.05	0.02	-11.1	3.7	0.1	63.5	0.45	8.78E-06
59			-10.7	9.3	0.09	54.3	0.23	1.16E-06
60			-10	7.4	0.12	60.2	0.31	1.90E-06
61	0.05	0.02	-11.7	73.3	0.37	62.3	0.17	1.13E-07
62	0.04	0.02	-10.9	68.7	0.34	66	0.07	6.38E-08
63			-10.7	14.7	0.11	47.8	0.99	1.70E-07
64			-12.1	92.1	0.46	57.8	0.12	9.20E-08
65			-7.5	1.2	0.09	49.9	1.23	1.09E-06
66			-10.5	7.1	0.11	65.5	1.69	1.46E-06
67			-10.5	7.5	0.11	84.1	0.48	1.57E-07
68			-9.7	13.3	0.12	60	0.27	3.83E-07
69			-8.2	1.9	0.09	27.8	0.97	2.19E-06
70			-10.6	2.2	0.1	29	0.04	9.91E-05
71			-11.7	2.6	0.1	51.5	0.04	1.03E-04
72	0.05	0.02	-9.9	1.8	0.09	13.6	0.31	6.24E-05
73	0.06	0.02	-8.5	3	0.1	40.5	0.06	1.89E-05
74	0.09	0.03	-12.7	3.8	0.13	68.2	0.07	1.78E-05
75	0.06	0.02	-12.6	1.8	0.09	93.4	0.01	1.24E-05
76	0.05	0.02	-12	2	0.09	89.5	0.04	9.49E-06
77	0.06	0.02	-12.8	2.2	0.09	97.6	0.09	1.06E-06
78	0.05	0.02	-13.1	45.1	0.22	104.7	0.07	2.19E-07
79	0.11	0.02	-	-	-	9.2	0.38	-

N.D: below detection limit; not analysed N.C: not correct

*: measured by accelerator mass spectrometer at ANU (Australian National University), Canberra

**: We used the un-fractionated excess air model to correct for excess air, based on Ne concentration and the He/Ne ratio in the dry air alone (Torgersen et al., 1978). We corrected the ^4He concentration only for samples containing excess air based on the dissolved Ne concentration (1.78×10^{-7} ccSTP/g) in distilled water at 2 a He/Ne ratio of 0.288.

Table 3 Geochemical, radiological, and isotopic data from rock samples in the Great Artesian Basin, for estimation of $^{36}\text{Cl}/\text{Cl}$ ratios, $^3\text{He}/^4\text{He}$ ratios and in-situ ^4He production rates.

Drill-hole names	Lithostratigraphic unit	Drill-core depths (m)	Sample numbers	U (mg/Kg)	Th (mg/Kg)	Li (mg/Kg)	n flux (n/cm2 s)	36Cl/Cl	3He/4He	4He production (ccSTP/cm3 water y)
Tieyon Cu	Algebuckii Sandstone	93.7-135.4	5	2.8±1.2	9.64±5.1	15.42±4.1	2.40E-05	1.10E-14	4.32E-09	3.10E-13
	Westbourn Cadna-owie Fm	206-216	2	7.3±3.7	16.6±4.4	60.75±51.4	6.70E-05	3.06E-14	2.15E-08	6.06E-13
Toodla 01		273.7	1	2	10.4	33.6	2.80E-05	1.28E-14	1.24E-08	2.42E-13
	Algebuckii Sandstone	284.6-319	4	1.1±0.5	4.5±3.2	16.5±12.2	1.30E-05	5.94E-15	5.87E-09	1.32E-13
GSQ Mam	Cadna-owie Fm	725.06-750	4	1.1±0.5	6.1±4.2	21.3±9.5	1.60E-05	7.31E-15	7.93E-09	1.38E-13
	Hooray Sandstone	765.4-817	6	1.7±1.2	8.8±6.2	31.3±24.8	2.40E-05	1.10E-14	1.17E-08	2.14E-13
BHP BH/V	Algebuckii Sandstone	167.1 - 171.2	2	0.9±0.1	3.2±0.4	7.8±1.7	1.00E-05	4.57E-15	2.78E-09	1.01E-13
	Proterozoic	175.2-176	1	1.6	0.9	22.1	1.04E-05	4.75E-15	7.52E-09	9.80E-14
GSQ Wyatt	Cadna-owie Fm	422.4 - 436	1	0.9	4.4	14.2	1.20E-05	5.48E-15	5.20E-09	1.05E-13
	Hooray Sandstone	501.6 - 648.7	3	1.2±0.7	8.5±7.3	11.3±1.0	2.03E-05	9.28E-15	4.23E-09	1.82E-13
	Early Jurassic	822.8 - 844	1	0.5	2	15.9	6.00E-06	2.74E-15	5.80E-09	5.28E-14

For calculation purposes, the density of rock is 2.6 g/cm³ for sandstone, 2.4 for other lithologies and the effective porosity is 20 percent